Mechanisms of Autophagy

Nobuo N. Noda[1,2] and Fuyuhiko Inagaki[2,3]

[1]Institute of Microbial Chemistry (BIKAKEN), Tokyo 141-0021, Japan; email: nn@bikaken.or.jp

[2]CREST, Japan Science and Technology Agency, 7, Gobancho, Chiyoda-ku, Tokyo 102-0076, Japan

[3]Faculty of Advanced Life Science, Hokkaido University, Sapporo 001-0021, Japan; email: finagaki@pharm.hokudai.ac.jp

Keywords

Abstract

The formation of the autophagosome, a landmark event in autophagy, is accomplished by the concerted actions of Atg proteins. The initial step of starvation-induced autophagy in yeast is the assembly of the Atg1 complex, which, with the help of other Atg groups, recruits Atg conjugation systems and initiates the formation of the autophagosome. In this review, we describe from a structural-biological point of view the structure, interaction, and molecular roles of Atg proteins, especially those in the Atg1 complex and in the Atg conjugation systems.

Contents

INTRODUCTION

Autophagosome:
a double-membrane organelle that emerges and sequesters cytoplasmic components during autophagy

Atg:
autophagy-related proteins

PI3K:
phosphatidylinositol 3-kinase

Pre-autophagosomal structure (PAS): a perivacuolar structure observed in yeast to which most Atg proteins localize and generate autophagosomes

Autophagy is an intracellular degradation system conserved among eukaryotes (74). The landmark event in autophagy is the generation of a double-membrane structure called the autophagosome. When autophagy is induced by starvation, a membrane sac called an isolation membrane appears and expands into an autophagosome. During this process, a portion of the cytoplasm including proteins and organelles is confined to the lumen of the autophagosome, and upon fusion between an autophagosome and a lysosome (or a vacuole in the case of yeast and plants), the inside contents are degraded by lysosomal hydrolases.

Using budding yeast, *Saccharomyces cerevisiae*, researchers have identified many autophagy-related (Atg) proteins that function in autophagy (51, 117, 118). Among these, 18 Atg proteins in six distinct groups help form the autophagosome: the Atg1 complex, the transmembrane protein Atg9, an autophagy-specific phosphatidylinositol 3-kinase (PI3K) complex, the Atg2-Atg18 complex, and the Atg8 and Atg12 conjugation systems (74, 79) (**Figure 1**). These six functional groups are localized to the pre-autophagosomal structure (or phagophore assembly site, PAS) and cooperate to generate autophagosomes (111, 113, 114). A systematic and quantitative analysis using fluorescence microscopy established a hierarchy map of these six groups involved in PAS assembly (113) (**Figure 1**). The most upstream and downstream groups in the map are the Atg1 complex and the Atg8 and Atg12 conjugation systems, respectively, and they are linked to each other through the other three Atg groups (74, 114). Most of these core Atg proteins and their interactions have been conserved evolutionarily, suggesting that the basic mechanism of autophagosome formation is also evolutionarily conserved.
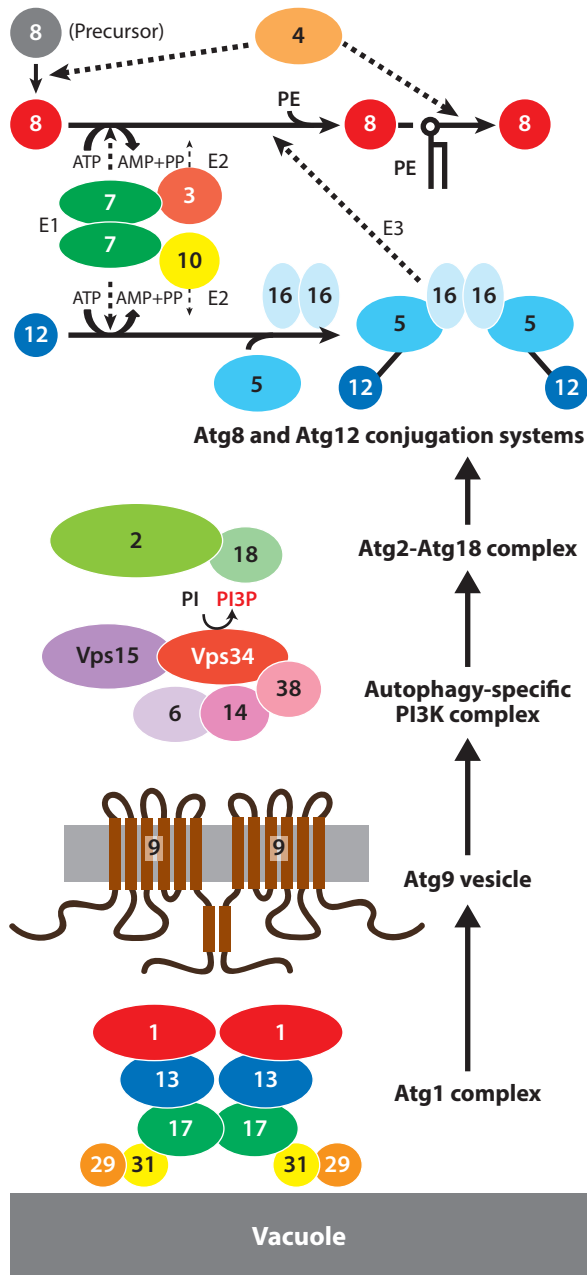
Figure 1

The six Atg groups involved in autophagosome formation. Six Atg groups target a perivacuolar site in a hierarchical manner. Abbreviations: PE, phosphatidylethanolamine; PI3K, phosphatidylinositol 3-kinase; PI3P, phosphatidylinositol 3-phosphate.

Many recent reviews on the physiology and cell biology of autophagy (59, 60, 70, 74, 98), as well as on the structural biology of autophagy (33, 52, 84), have been published. In this review, we focus on the core Atg proteins, especially those forming the Atg1 complex and the two Atg conjugation systems, and update from a structural-biological point of view the current understanding of their structure and molecular role in autophagosome formation.

Atg1 COMPLEX: THE INITIATOR OF AUTOPHAGOSOME FORMATION

Formation of the PAS is critical for initiating the formation of the autophagosome (111). Upon starvation, the first step in creating the PAS is the assembly of the Atg1 complex (113). Atg1 is a serine-threonine kinase and its kinase activity is essential for the formation of the autophagosome (43). In *S. cerevisiae*, Atg1 forms a complex with four other Atg proteins, Atg13, Atg17, Atg29, and Atg31, upon starvation (7, 46). The Atg1-Atg13-Atg17-Atg29-Atg31 complex (referred to as the Atg1 complex hereafter) recruits Atg9 and the autophagy-specific PI3K complex, which in turn recruit the Atg2-Atg18 complex and the Atg conjugation systems, and thus complete PAS assembly (113) (**Figure 1**). Formation of the Atg1 complex enhances the kinase activity of Atg1, which is also important for the progress of autophagy (43). The elevated kinase activity itself is not required for recruiting downstream Atg proteins to the PAS, but it is required for cycling the Atg proteins between the PAS and other membrane compartments (97).

Architecture of Atg1

Atg1 can be structurally divided into three regions: an N-terminal kinase domain (KD); a C-terminal globular domain; and an intrinsically disordered region (IDR), which connects the first two (**Figure 2a**). The structure of the Atg1 KD, which has not been determined experimentally, is predicted to belong to a protein kinase superfamily fold owing to the high sequence similarity. Thr226 and Ser230 (residue types and numbers in this review refer to *S. cerevisiae* Atg when not otherwise specified) in the activation loop of the Atg1 KD are autophosphorylation sites and their phosphorylation is critical for both kinase activity and autophagy (48, 128). Yeh et al. (127) proposed a model in which Atg13 induces dimerization of Atg1, which promotes autophosphorylation of Thr226 and thus activates the kinase activity of Atg1. Additional structural studies of the Atg1 KD are needed to validate these models.

X-ray crystallography has determined the structure of the C-terminal domain (CTD) as a complex with the Atg1-binding region of Atg13 (13) (**Figure 2a**). The CTD of Atg1 consists of

---

Figure 2

Structure and phosphoregulation of the Atg1 complex. (*a*) Architecture of Atg1 and its interaction with Atg13. The Atg1^{tMIT}-Atg13^{MIM} complex model was generated using PDB ID 4P1N. All structural models in this article were prepared using the program PyMOL. The IDRs are indicated by curved lines. The inset denotes the region shown in panel *d*. (*b*) Structure of Atg13^{HORMA} and how it compares with Mad2. Structural models for the HORMA domains of Atg13 and Mad2 (closed and open conformations) were generated using PDB IDs 4J2G and 1GO4, respectively. (*c*) Architecture of the Atg17-Atg29-Atg31 complex. The structure of the Atg13^{17BR}-Atg17-Atg29-Atg31 complex (PDB ID 4P1W) was used to generate models. The inset denotes the region shown in panel *e*. (*d*) Close-up view of the interaction between Atg1^{MIT2} and Atg13$^{MIM(N)}$. (*e*) Close-up view of the interaction between Atg13^{17BR} and Atg17; broken lines indicate possible hydrogen bonds. Abbreviations: AIM, Atg8-family-interacting motif; C, carboxy termini; HORMA, Hop1p, Rev7p, and Mad2; IDR, intrinsically disordered region; MIM, MIT-interacting motif; MIT, microtubule-interacting and transport domain; N, amino termini; P, phosphorylation.

six α-helices, which fold into two three-helix bundles, and these two bundles interact to form one globular fold. Each bundle resembles a microtubule-interacting and transport (MIT) domain—hence the names MIT1 and MIT2. The MIT domains are often observed in proteins involved in membrane traffic such as the multivesicular body pathway, and they function as a binding module that connects proteins (34). Tandem MIT domains (tMIT) of Atg1 are responsible for binding Atg13, and their mode for recognizing Atg13 is similar to how other MIT domains recognize

their targets (described below). In addition to binding Atg13, the CTD of Atg1 was suggested to bind Atg11 (65), the scaffold protein essential for selective autophagy, such as the Cvt (cytoplasm-to-vacuole targeting) pathway, and membranes, especially those with high curvature (96). The Atg11-binding site, which is distinct from the Atg13-binding site (the first and the third α-helices of MIT2, as described below), was assigned to be the second α-helix of MIT2 (65) and thus Atg11 might not compete with Atg13 for Atg1 binding. The structure of Atg1 tMIT does not possess a surface suitable for sensing membrane curvature; thus, further studies are needed to determine its membrane-related functions.

The IDR of Atg1, which consists of ~300 residues, connects the KD and the tMIT. It remains to be elucidated whether the Atg1 IDR connects them as a random coil and whether the relative positioning of the two globular domains is completely variable or fixed to some extent. The Atg1 IDR contains an abundance of serines and threonines, many of which are phosphorylated by various kinases (5, 16, 24, 48, 104). The roles of phosphorylation at these sites are largely unknown; however, Budovskaya et al. (5) have shown that Ser508 and Ser515 in the Atg1 IDR are phosphorylated by the cAMP-dependent protein kinase and that these phosphorylations regulate the localization of Atg1 to the PAS but not its kinase activity. Structural information on Atg1, including its IDR, is urgently required to establish the biological significance of each phosphorylation site in the IDR. The Atg1 IDR possesses an Atg8-family-interacting motif (AIM) (85) and directly interacts with Atg8 (55, 78). This interaction is dispensable for targeting Atg1 to PAS but essential for tethering Atg1 to the isolation membrane. Although the Atg1-Atg8 interaction is important for efficient autophagy, the role of Atg1 in relation to isolation membranes remains to be established.

Architecture of Atg13

Atg13 can be structurally divided into two regions: an N-terminal globular domain and a C-terminal IDR. X-ray crystallography has determined the structure of the NTD of Atg13 (37) (**Figure 2b**). The core of the NTD consists of a five-stranded antiparallel β-sheet and four α-helices on the same side of the sheet. A smaller three-stranded antiparallel β-sheet is located at the C-terminal side of the core. The topology of the core structure is essentially identical to that of the Hop1p, Rev7p, and Mad2 (HORMA) domains (2), which is why the NTD of Atg13 was named HORMA. Structural studies of the Mad2 HORMA domain showed that Mad2 possesses an open conformation (o-Mad2) and a closed conformation (c-Mad2), and that ligand binding shifts the equilibrium to c-Mad2 (63) (**Figure 2b**). The Atg13 HORMA domain is topologically similar to c-Mad2, and it remains to be elucidated whether the Atg13 HORMA domain also has two conformations. In the crystal structure of the Atg13 HORMA domain, a sulfate ion was bound in proximity to the basic side chains of two arginines that are located at the core β-sheet and at the loop region, called the safety-belt (37). In the case of Mad2, the safety-belt undergoes a large conformational change upon ligand binding and locks the ligand by functioning as a fastened safety-belt (63). Because sulfate ions are often observed in the phosphate-binding pocket of a protein, scientists speculated that phosphorylated serine and threonine residues in Atg13 or an Atg13-binding protein could bind to the two arginines in a manner similar to that of the sulfate ion, and that this interaction could switch the conformation of the Atg13 HORMA domain from open to closed as in the case of Mad2. However, the conservation of the two arginines is restricted to species closely related to *S. cerevisiae*; they are not conserved in mammalian Atg13 (37). The Atg13 HORMA domain is necessary for targeting the autophagy-specific PI3K complex, but not the Atg1 complex, to the PAS (37). However, direct interaction between the Atg13 HORMA domain and the PI3K complex has not been observed. In the case of mammals, the Atg13 HORMA domain

binds Atg101; however, Atg101 is not conserved in budding yeast (29, 67). To establish the specific function of the Atg13 HORMA domain in autophagy, its binding partner(s) must be identified.

The Atg13 IDR has been predicted to be quite long (∼470 amino acids) and contains abundant serines and threonines, many of which are phosphorylated by various kinases (4, 13, 24, 32, 44, 61, 104–106). The Atg13 IDR is responsible for binding both Atg1 and Atg17 (8, 43); thus phosphorylation at the Atg13 IDR regulates autophagy by changing the affinity of Atg13 to Atg1 and Atg17 (described below). The Atg1-binding region was assigned to the ∼60-residue region (residues 460–521), whereas only a 13-residue region (residues 424–436) is sufficient for binding Atg17 (13). Circular dichroism spectroscopy confirmed that the Atg1-binding region is intrinsically disordered when in free form, whereas two α-helices were induced upon Atg1 binding (13) (described below). The Atg17-binding region is too short to contain a globular fold. Because the Atg13 IDR is phosphoregulated by nutrient conditions, Jao et al. (37) speculated that a phosphorylated IDR could bind to the two arginines in the HORMA domain of the same protein by which Atg13 is fixed to a closed conformation and that starvation-induced dephosphorylation of IDR releases the closed conformation, enabling the HORMA domain to bind downstream factors. However, no interaction between the IDR and the HORMA domain of Atg13 has been observed. A structural analysis of full-length Atg13 is needed to substantiate these speculations.

Architecture of the Atg17-Atg29-Atg31 Complex

Atg17, Atg29, and Atg31 form a 2:2:2 stable complex in vitro (41). Further, they constitutively form a complex with each other irrespective of nutrient conditions in vivo (41). In total, they may be considered as one structural unit. The crystal structure of full-length Atg17 with full-length Atg31 and Atg29 lacking its C-terminal IDR has been determined (96) (**Figure 2c**). The Atg17 protomer consists of four α-helices, which fold into a crescent-like structure, and Atg17 dimerizes via its C-terminal region, which results in its unique S-shaped architecture. Single-particle electron microscopy has also shown that Atg17 is S-shaped when in complex with Atg29 and Atg31, but that in free form Atg17 has a more elongated conformation that is rodlike rather than crescent-like (9, 65).

Atg31 has a β-sandwich fold consisting of eight β-strands, one of which is derived from the N-terminal region of Atg29, and thus Atg31 appears to not retain its folded structure in the absence of Atg29 (96) (**Figure 2c**). In addition to the β-sandwich fold, Atg31 has one α-helix at the C terminus, which binds tightly to Atg17 by forming an intermolecular four-helix bundle with the three α-helices of Atg17 (96). In contrast, the β-sandwich moiety of Atg31 showed little interaction with Atg17. Atg29 consists of the N-terminal β-strand, which forms the Atg31 β-sandwich fold; three α-helices; and the C-terminal IDR (96). Both Atg29 and Atg31 bind to the middle of the concave surface of the crescent-like fold of Atg17 mainly via the C-terminal helix of Atg31. Atg29 does not directly interact with Atg17 in the crystal structure, although there remains a possibility that the Atg29 IDR directly interacts with Atg17.

The Atg29 IDR contains many serine and threonine residues that are phosphorylated upon starvation (65). Although deletion of the Atg29 IDR did not impair autophagic activity, unphosphorylatable mutations at the Atg29 IDR severely impaired autophagy (65). These observations suggest that the Atg29 IDR inhibits autophagy and that phosphorylation of the IDR impairs its inhibiting activity and promotes autophagy. The molecular mechanism of the inhibitory activity of the Atg29 IDR remains to be established. Atg11 interacts directly with the phosphorylated IDR of Atg29, which promotes the recruitment of the Atg17-Atg29-Atg31 complex to the PAS in cells lacking Atg1 and Atg13 (65). However, Atg11 is not required for the assembly of the

Atg1 complex under starvation or for starvation-induced autophagy (43, 46, 49). To better understand this process, the significance of the Atg11-Atg29 interaction in autophagy requires further investigation.

Structural Basis of the Atg1-Atg13 Interaction

In general, proteins that interact with MIT domains utilize an MIT-interacting motif (MIM) (34). There are several types of MIMs, most of which have a helical conformation and form an intermolecular helix bundle by binding to the groove formed between two α-helices of the MIT (34). The Atg1-binding region of Atg13 also binds to Atg1^{tMIT} with a helical conformation: The N-terminal helix binds to the groove formed between the first and third helices of Atg1^{MIT2}, whereas the C-terminal helix binds to the groove formed between the second and third helices of Atg1^{MIT1} (13); the N- and C-terminal helices of Atg13 are called MIM(N) and MIM(C) (**Figure 2a**). The buried surface between Atg13$^{MIM(C)}$ and Atg1^{MIT1} is larger than that between Atg13$^{MIM(N)}$ and Atg1^{MIT2}; nevertheless, in vitro studies have shown that the affinity between Atg1 and Atg13 is endowed primarily by the Atg1^{MIT2}-Atg13$^{MIM(N)}$ interaction and that the Atg1^{MIT1}-Atg13$^{MIM(C)}$ interaction secondarily reinforces it (13). Consistently, Phe468 and Leu472 in Atg13$^{MIM(N)}$, which are deeply bound to the hydrophobic groove of Atg1^{MIT2} (**Figure 2d**), are essential for the interaction with Atg1 (13, 55).

Structural Basis of the Atg13-Atg17 Interaction

The minimum Atg17-binding region (17BR) of Atg13 is composed of 13 amino acids. Crystallographic study of Atg13^{17BR} in complexes with the Atg17-Atg29-Atg31 complex showed that only six residues in 17BR had a defined electron density, and thus modeling was performed on these six residues (13) (**Figure 2e**). Atg13^{17BR} is bound to the hydrophobic groove of the N-terminal region of Atg17 using the two hydrophobic side chains Phe430 and Ile433. Further, Ser428 and Ser429 of Atg13 form hydrogen bonds with Asp247 of Atg17. Alanine substitution at these hydrophobic residues and serines in Atg13 severely impairs the interaction between Atg13^{17BR} and Atg17 (13). Further, the D247A mutation in Atg17 severely impaired both the interaction of full-length Atg13 with Atg17 and the autophagy progression in vivo (13). This finding suggests that the Atg13^{17BR}-Atg17 interaction observed in the crystal structure is essential for the Atg13-Atg17 interaction and for autophagy.

The Atg13 IDR is very long (as many as ~470 residues), and regions in the IDR other than 17BR might also be involved in the interaction with Atg17. An in vitro study showed that mutations at 17BR did not completely impair the interaction between full-length Atg13 and Atg17 (Y. Fujioka & N.N. Noda, unpublished observations). A previous study reported that a single point mutation at Cys24 with arginine in Atg17 impaired the interaction with Atg13 (39). The Cys24 is located at the N-terminal region of Atg17 but is not involved in the formation of the binding site for Atg13^{17BR} (**Figure 2e**). Because the side chain of Cys24 is buried and surrounded by hydrophobic residues, its arginine substitution may have remotely disturbed the conformation of the Atg13^{17BR}-binding site. Further characterization of the Atg13 IDR other than in 17BR and MIM may provide more information on the functions of Atg13.

Dephosphorylation of Atg13 Leads to the Formation of the Atg1 Complex

Autophagy is strongly induced by starvation and is believed to be regulated by the nutrient sensor TORC1 [target of rapamycin (Tor) complex 1] (87). Under nutrient-rich conditions, TORC1 is

active and directly phosphorylates Atg13. Starvation inhibits TORC1 activity, leading to immediate dephosphorylation of Atg13 possibly by an unidentified phosphatase(s) (43). The following events that initiate autophagy are currently unconfirmed. One possible model is that dephosphorylated Atg13 increases the affinity of Atg13 to both Atg1 and Atg17, which then leads to the formation of the Atg1 complex and to PAS assembly (13, 43). Eight serines in the Atg13 IDR were identified as TORC1-phosphorylating sites responsible for regulating autophagy, and importantly, overexpression of Atg13 with alanine substitution at all eight serines induced autophagy even under growth conditions (44). These data strongly suggest that dephosphorylation at the Atg13 IDR is sufficient to induce autophagy. Further, three serines in the Atg13 IDR were identified as phosphorylation sites by cAMP-dependent protein kinase, and their alanine substitution promoted PAS targeting of Atg13, possibly by interacting with Atg17 (106). However, owing to a lack of structural information, these studies did not establish the molecular mechanisms of phosphorylation-mediated regulation of the Atg1 complex assembly. Via structure-based analysis we recently identified specific serines in the Atg13 IDR that are directly involved in the Atg13-Atg17 interaction (13).

Both Atg13$^{MIM(C)}$ and Atg13^{17BR}, which are responsible for binding Atg1 and Atg17, respectively, contain serines that are phosphorylated under nutrient-rich conditions and dephosphorylated upon treatment with rapamycin. Aspartate mutation at five serines in Atg13$^{MIM(C)}$ that mimic phosphorylation moderately weakened the Atg1-Atg13 interaction, whereas aspartate mutation at Ser429 in Atg13^{17BR} severely impaired the Atg13-Atg17 interaction both in vitro and in vivo (13). Consistent with this finding, autophagy was partially and severely impaired when these serines were mutated to aspartate in Atg13$^{MIM(C)}$ and Atg13^{17BR}, respectively (13). Ser429 of Atg13 forms an important hydrogen bond with Asp247 of Atg17, as described above (**Figure 2e**). Phosphorylation at Ser429 would not only destroy the hydrogen bond but also cause electrostatic repulsion between the introduced phosphate group and Asp247, which could account for the complete inhibition of the Atg13-Atg17 interaction by an S429D mutation. Phosphorylation at Ser428 would also inhibit the interaction in a similar mechanism. In contrast, the Atg1-Atg13 interaction, which is mediated mainly by Atg13$^{MIM(N)}$, is regulated by multiple phosphorylations at Atg13$^{MIM(C)}$. Because Atg13$^{MIM(C)}$ enhances the Atg1-Atg13$^{MIM(N)}$ interaction, phosphorylation at Atg13$^{MIM(C)}$ is not sufficient to completely destroy the Atg1-Atg13 interaction. This mild regulation of the Atg1-Atg13 interaction may be needed to retain a small population of the Atg1-Atg13 complex required for the Cvt pathway under nutrient-rich conditions. This is in contrast to the Atg13-Atg17 interaction, which is not required for the Cvt pathway; thus, its complete inhibition would be possible. Recently, Kraft et al. (55) reported that Atg13 constitutively forms a complex with Atg1 and that the phosphorylated state of Atg13 does not affect formation of the complex. Although the exact reason for the various different observations remains to be elucidated, one possible explanation is that the formation of the Atg1-Atg13 complex is not fully regulated by the nutrient conditions, which makes it technically difficult to detect starvation-dependent increases in the Atg1-Atg13 complex. The data reported so far may indicate that the starvation-dependent interaction of Atg13 with Atg17, rather than the interaction of Atg13 with Atg1, is more important for fully regulating autophagy.

The Mammalian ULK1 Complex

In higher eukaryotes such as mammals, ULK1 and ULK2 are the orthologs of yeast Atg1 (69). ULK1 and ULK2, along with several other proteins including mammalian Atg13 (6, 15, 27, 38); RB1-inducible coiled-coil protein 1 (RB1CC1), also known as FIP200 (15, 20, 27, 38); and Atg101 (29, 67), contribute to the initial step of autophagosome formation in complexes. RB1CC1 has been suggested to be a functional homolog of yeast Atg17 on the basis of observations that it directly

interacts with Atg13, and is predicted to possess coiled coils similar to those in Atg17, although little sequence homology is observed between RB1CC1 and Atg17 (20). The C-terminal region of RB1CC1 shows sequence homology to that of Atg11, suggesting that RB1CC1 may be a hybrid homolog of yeast Atg11 and Atg17. The mammalian ULK1/2 complex lacks Atg29 and Atg31 counterparts but possesses Atg101, which is not conserved in budding yeast. Fission yeast conserves an Atg101 homolog, Mug66, but lacks Atg29 and Atg31 (29, 109). The Atg29-Atg31 pair and Atg101 appear to be mutually exclusive throughout evolution; thus, it could be speculated that they play equivalent roles. However, although the Atg29-Atg31 pair directly interacts with Atg17 but not with Atg13, the binding partner of Atg101 is Atg13 and not the Atg17 counterpart, RB1CC1. Further, the structure of Atg101 was predicted to be similar to that of the HORMA domains (23), which is quite different from the structure of the Atg29-Atg31 pair (96) (**Figure 2**). Another important difference from the yeast Atg1 complex is that the ULK1/2 complex exists constitutively and its formation is not regulated by nutrient conditions (69). However, mammalian Atg13 is also phosphorylated by mTORC1, suggesting a general regulatory mechanism of starvation-induced autophagy that is at least partly shared between mammals and yeast.

Downstream Factors of the Atg1 Complex

Atg9, present in single-membrane vesicles with a diameter of 30–60 nm called the Atg9 vesicles, travels between the PAS and other membrane compartments (126). Although there are no structural studies of Atg9, Atg9 is predicted to have six transmembrane helices followed by a coiled coil and to be present as a homodimer via the dimerization of the coiled coil (21). Targeting Atg9 to the PAS requires the Atg1 complex but not the kinase activity of Atg1 (97, 113). Atg9 is a direct target of Atg1 and phosphorylated Atg9 is responsible for efficiently recruiting Atg8 and Atg18 to the PAS (93). However, how Atg9 targets the PAS and recruits downstream factors to the PAS and how Atg1-mediated phosphorylation regulates Atg9 function await further study, especially a structural analysis of Atg9.

The autophagy-specific PI3K complex, consisting of Vps34, Vps15, Atg6/Vps30, Atg14, and Atg38, targets the PAS via the Atg1 complex (1, 47). Vps34 is the catalytic subunit of the PI3K complex; Vps15, Atg6/Vps30, and Atg14 regulate the activity and the localization of Vps34; and Atg38 may be important for the integrity of the PI3K complex (1). The PI3K complex targets the PAS depending on both Atg9 and the Atg1 complex (113). Thus far we know the Atg14 complex, the BARA domain of Atg6, and the HORMA domain of Atg13 are required for the PI3K complex to target the PAS (37, 82, 89). However, a direct interaction(s) that connects the PI3K complex to Atg9 or to the Atg1 complex has not been reported. Further investigations are required to elucidate how the PI3K complex targets the PAS.

Atg CONJUGATION SYSTEMS: THE WORKERS THAT EXPAND ISOLATION MEMBRANES

In autophagy, there are two ubiquitin-like conjugation systems: the Atg8 and Atg12 systems (90) (**Figure 1**). The Atg12 system contains five Atg proteins: Atg5, Atg7, Atg10, Atg12, and Atg16 (72, 73, 103). Atg12 is activated by Atg7, an E1-like enzyme (73), and is then transferred to Atg10, an E2-like enzyme (103). Finally, the C-terminal glycine of Atg12 is conjugated to the side chain of Lys149 of Atg5 (73). The unique feature of the Atg12 system is that E3 enzymes are not required for this conjugation reaction. There is no deconjugation enzyme, and the Atg12-Atg5 conjugate is formed constitutively in vivo. The Atg12-Atg5 conjugate further forms a complex

with a dimeric protein, Atg16 (Atg16L in the case of mammals and plants), with which Atg5 interacts noncovalently (12, 71, 72).

The Atg8 system contains four Atg proteins: Atg3, Atg4, Atg7, and Atg8 (35) (**Figure 1**). Nascent Atg8 is processed by Atg4, a cysteine protease, to expose a glycine residue at its C terminus (50). The processed Atg8 is then activated by Atg7, the same E1-like enzyme as in the Atg12 system, and transferred to Atg3, an E2-like enzyme (35). Finally, the C-terminal glycine of Atg8 is conjugated to the amine moiety of phosphatidylethanolamine (PE) (35). The final step in conjugation requires the E3-like Atg12-Atg5-Atg16 complex, the product of the Atg12 system (18). Atg4 also works as a deconjugation enzyme that cleaves Atg8-PE so that Atg8 may be reused. The unique feature of the Atg8 system is that Atg8 is conjugated to a lipid, not to a protein.

Atg8: A Ubiquitin-Like Protein

X-ray crystallography and NMR have shown that Atg8 and its homologs in mammals, *Bombyx mori*, *Plasmodium falciparum*, and *Trypanosoma brucei* share a similar structure composed of a ubiquitin-core fold and two α-helices at its N-terminal side (17, 30, 54, 58, 83, 94, 107) (**Figure 3a**). The two α-helices endow Atg8 with two unique properties. First, Atg8-PE-containing liposomes are tethered together via the self-association property of Atg8-PE in vitro, for which the two α-helices are essential (77, 120). Second, there is a deep hydrophobic pocket, called the W-site, between the two α-helices and the ubiquitin core. The W-site, together with another hydrophobic pocket in the ubiquitin core, called the L-site, plays an important role in selective autophagy. The Cvt pathway is a well-characterized example of selective autophagy in which vacuolar enzymes such as aminopeptidase I (Ape1) and α-mannosidase (Ams1) are selectively packaged in an autophagosome-like structure called a Cvt vesicle and delivered into the vacuole under nutrient-rich conditions (64). The adaptor protein Atg19 links the vacuolar enzymes to the Cvt vesicle by interacting with both the vacuolar enzymes and Atg8 (102), the latter of which is mediated by an AIM (83, 85). The Atg19 AIM has a WEEL sequence and uses the side chains of Trp and Leu in the sequence to bind to the above-mentioned W- and L-sites on Atg8 (83) (**Figure 3a**). In addition, the backbone of the AIM forms a parallel β-sheet with Atg8 β2, which is similar to the interaction between the SUMO and SUMO-interacting motif (22). Mammalian Atg8 homologs such as LC3 also recognize a WXXL-like sequence in a manner similar to that of Atg8; thus, such a sequence in mammals is called the LC3-interacting region (LIR) (36, 83, 92). The AIM/LIR is conserved in other adaptor proteins such as Atg32, Atg34, Atg36, and Cue5 in yeast and p62, Nix, and Tollip in mammals, and the interaction between the AIM/LIR and Atg8-family proteins is also conserved (53, 62, 75, 88, 92, 112). Further, AIM/LIR is observed in core Atg proteins such as Atg1, Atg3, Atg12, and mammalian Atg4B and Atg13, and appears to tether these factors to autophagic membranes via the interaction with Atg8-PE (45, 55, 78, 100, 110, 124).

Atg4: Processing and Deconjugation

Atg4 mediates both processing of nascent Atg8 and deconjugation of Atg8-PE conjugates (40, 50). Structural studies of the human Atg4 ortholog, HsAtg4B, in free form and in complex with LC3 have been published (57, 100, 108) (**Figure 3b**). HsAtg4B has a papain fold with a catalytic triad consisting of Cys74, Asp278, and His280. A notable feature is that the catalytic site of HsAtg4B is buried, covered by the regulatory loop, Trp142, and the N-terminal tail (108) (**Figure 3b**, free HsAtg4B), making it inaccessible in the free form. The crystal structure of HsAtg4B in complex with LC3 showed that HsAtg4B binds two LC3 proteins; one LC3 binds
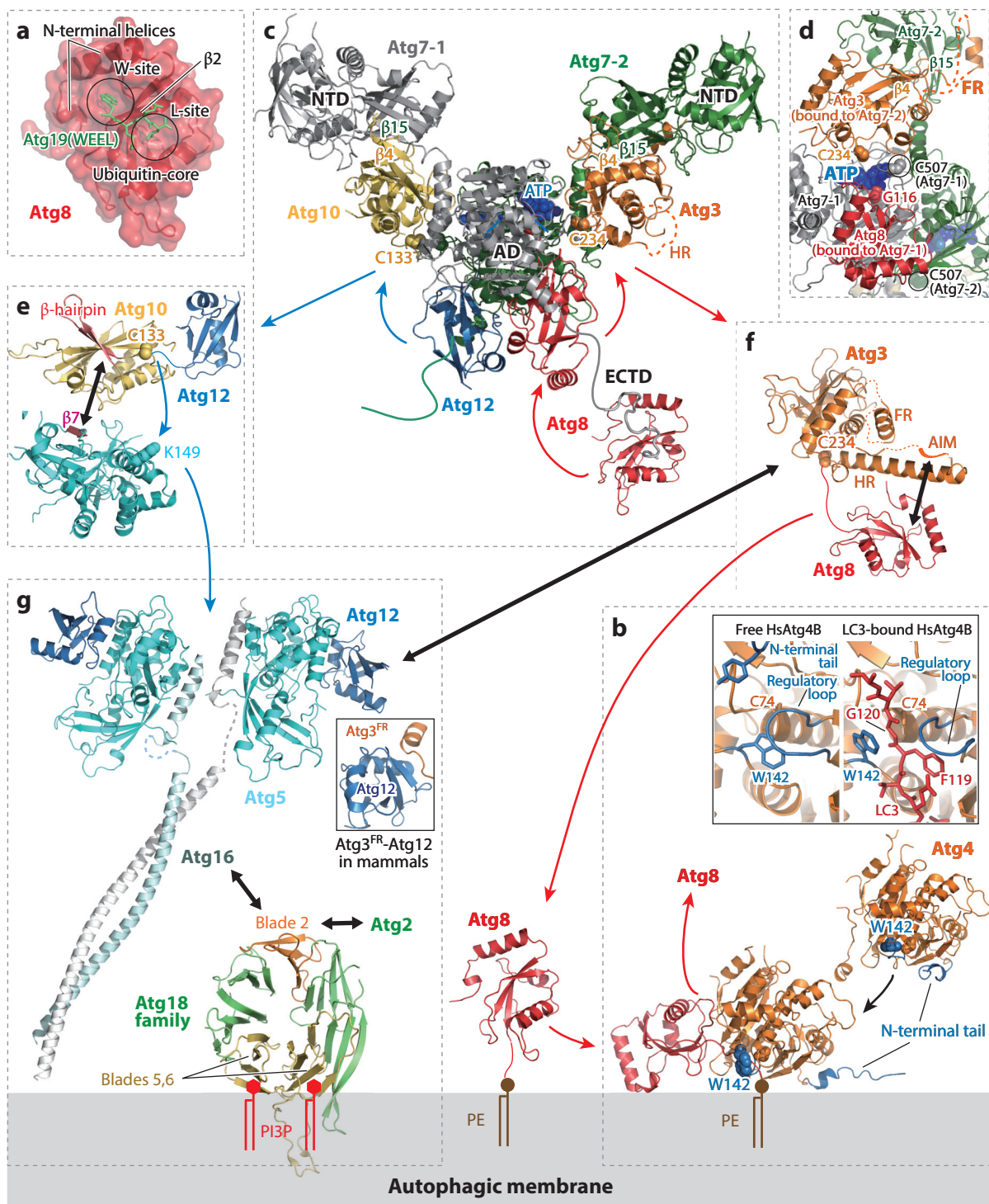
to the LIR in the N-terminal tail, which opens the exit of the catalytic site, and the other LC3 binds to the papain fold and extends the C-terminal tail into the cleft to expose the scissile bond to the catalytic cysteine, Cys74 (100). A remarkable feature is the large conformational change around the regulatory loop and Trp142: The insertion of the C-terminal tail, especially Phe119, of LC3 dislocates the root of the regulatory loop and thereby disrupts the interaction between Trp142 and the regulatory loop (**Figure 3*b***, LC3-bound HsAtg4B). This disruption allows the C-terminal tail of the LC3 precursor to enter the catalytic site. Trp142 of HsAtg4B and Phe119 of LC3 are conserved, suggesting that these interaction modes are also evolutionarily conserved. The C-terminal LC3 peptide alone does not induce the conformational change, and both the ubiquitin core and the C-terminal tail are essential for LC3 to be processed by HsAtg4B.

Atg7: An Activating (E1-Like) Enzyme

The E1-like enzyme Atg7 first adenylates two ubiquitin-like proteins (Ubls), Atg8 and Atg12, consuming ATP, then forms a thioester intermediate with both, and finally transfers them to each cognate E2 enzyme, Atg3 and Atg10. X-ray crystallography of Atg7 has established the unique architecture of Atg7 (26, 86, 116) (**Figure 3*c***). Atg7 is composed of the NTD, the CTD, and a short linker that connects them. The CTD is subdivided into the adenylation domain (AD) and the extreme C-terminal domain (ECTD). The AD forms a homodimer whose architecture is similar to the heterodimeric architecture of the active and nonactive ADs in canonical E1 enzymes (26, 86, 101, 116). However, in addition to the AD, the structure of Atg7 is totally distinct from that of the canonical E1 enzymes in ubiquitin-related systems; Atg7 has neither a ubiquitin-fold domain nor a catalytic cysteine domain, which is conserved among canonical E1 enzymes. The NTD and ECTD of Atg7 have never been observed in other E1 enzymes, and these structural features suggest that Atg7 works by a mechanism different from that used by canonical E1 enzymes.

The crystal structure of the Atg7 CTD in complex with Atg8 and MgATP showed that Atg8 and MgATP are loaded on both CTDs within a dimer (26, 86), confirming that both activation domains are active. In contrast, in the case of canonical E1 enzymes, one of the activation domains is inactive. The catalytic cysteine in Atg7 is located on a crossover loop, which covers the Atg8-binding surface in the free form but shows a local conformation change and exposes the surface upon binding Atg8 (26, 86). Using hydrophobic residues (Ala75, Phe77, Phe79, Leu84, and Thr87), the ubiquitin core of Atg8 binds to the central β-sheet of the AD. The C-terminal tail of Atg8 extends under the

Figure 3

Structure and mechanism of the Atg conjugation systems. (*a*) Structure of Atg8 in complex with the WEEL sequence of Atg19 (PDB ID 2ZPN). (*b*) Structure of human Atg4B alone and in complex with LC3 (PDB ID 2CY7, 2ZZP). (*c*) Modeled structure of the Atg7-Atg3-Atg8-Atg10-Atg12 complex. The model was generated by superimposing the structures of the Atg7-Atg3 and Atg7-Atg10 complexes (PDB ID 4GSL, 4GSK) and plant Atg12b (PDB ID 1WZ3) on the structure of the Atg7-Atg8-MgATP complex (PDB ID 3VH4). The loop region containing Cys133 of Atg10 was derived from the Atg10 structure (PDB ID 4EBR). The model of Atg8 in complex with the loop of Atg7[ECTD] was generated using the NMR structure of the Atg8-Atg7[C30] complex (PDB ID 2LI5). One Atg7 protomer in complex with Atg8 and Atg10 is labeled Atg7-1 (*gray*); the other Atg7 protomer in complex with Atg3 and Atg12 is labeled Atg7-2 (*green*). (*d*) Close-up view of the catalytic site in panel *c*. Atg8 Gly116 and the side chains of Atg3 Cys234 and Atg7 Cys507 as well as ATP are shown with space-filling models. (*e*) Structure of Atg5 (PDB ID 2DYO) and Atg10 (PDB ID 2LPU). The side chains of Atg10 Cys133 and Atg5 Lys149 are shown with a space-filling model. (*f*) Structure of Atg3 (PDB ID 2DYT). The side chain of Atg3 Cys234 is shown with a space-filling model. (*g*) Structure of the Atg12-Atg5-Atg16 complex (PDB ID 3W1S, 3A7P) and the Atg18-family protein Hsv2 (PDB ID 3VU4). The interaction between Atg12 and Atg3[FR] (PDB ID 4NAW) is shown in the inset. Red and blue arrows indicate the flow of Atg8 and Atg12, respectively. The black double-headed arrow indicates possible interactions. Abbreviations: AD, adenylation domain; AIM, Atg8-family-interacting motif; ECTD, extreme C-terminal domain; FR, flexible region; HR, handle region; NTD, N-terminal domain; PE, phosphatidylethanolamine; PI3P: phosphatidylinositol 3-phosphate.

crossover loop and the C-terminal Gly116 of Atg8 is located around the bound MgATP and the catalytic cysteine, Cys507 (**Figure 3d**). This structure supports the idea that the adenylation of Atg8 Gly116 and its subsequent thioester formation with Atg7 Cys507 proceed with only a local conformational change in Atg7. This process is different for canonical E1 enzymes, in which a drastic domain rearrangement occurs during activation reactions (101). Although the C-terminal residues of the Atg7 ECTD were not visible in the crystal structure, they play an essential role in binding and activating Atg8 by Atg7. The NMR structure of Atg8 in complex with the C-terminal 30-residue peptide of Atg7 (Atg7 C30) showed that Atg7 C30 binds to the W- and L-sites in Atg8 with extensive hydrophobic and hydrophilic interactions, which are important for the activation reaction (86).

A two-step recognition model was proposed on the basis of these observations: Atg8 is first captured by the C-terminal tail of Atg7 and then recruited to the AD as in the crystal structure and from here the activation reaction proceeds (**Figure 3c**). Recognition and activation of another Ubl, Atg12, by Atg7 seem similar to that of Atg8 by Atg7 (see **Figure 3c** for a model of the Atg7-Atg12 complex), although a structural study has not been performed. Atg12 does not possess the W-site because the N-terminal helices are absent, suggesting that many of the interactions that Atg7 C30 forms with Atg8 may be impossible with Atg12. This implies that compared with Atg12, Atg8 may be more efficiently captured and activated by Atg7, which would be advantageous as autophagy requires a large amount of Atg8-PE but only a small amount of Atg12-Atg5 (28, 121).

Atg3 and Atg10: Conjugating (E2-Like) Enzymes

Atg8 or Atg12 bound to Atg7 via a thioester bond is transferred to the E2-like enzymes Atg3 or Atg10 to form the Atg8~Atg3 or the Atg12~Atg10 thioester intermediate, respectively (35). Atg3 and Atg10 share an E2-core fold that is somewhat different from that in canonical E2 enzymes: It lacks the C-terminal two α-helices. In addition, Atg10 possesses a characteristic β-hairpin that extends over the core β-sheet (25, 122, 125) (**Figure 3e**). Atg10 directly recognizes Atg5 at β7 using the β-hairpin and catalyzes the Atg12-Atg5 conjugation without an E3 enzyme (125). In addition to the E2-core fold, Atg3 has two unique insertions, a handle region (HR) and a flexible region (FR), giving Atg3 a hammer-like shape consisting of a head (E2 core) and a handle (HR) (122) (**Figure 3f**). Many of the residues forming the components of the protruding α-helix in the handle region are disordered in the crystal structure of the Atg3-Atg7 complex (42) (**Figure 3c**), suggesting that the unique structure of the handle region is possibly due to crystal contacts. Atg3^{FR} (residues 84–162) has a highly acidic character and most of its residues are intrinsically disordered. The handle region contains an AIM that binds to Atg8 (124), whereas the flexible region has a small α-helical region that binds to the Atg7 NTD (116, 122) (**Figure 3d**). The N-terminal region of Atg3, which is disordered in the crystal structure but is essential for autophagy, has been suggested to form an amphipathic helix and to bind membranes with high curvature (19, 80). However, the proper targeting of Atg3 to autophagic membranes requires the E3-like Atg12-Atg5-Atg16 complex in vivo (14).

The Structural Basis of the Transfer of Atg8 and Atg12 from Atg7 to E2 Enzymes

Data from recent crystallographic studies of the Atg7-Atg3 and Atg7-Atg10 complexes explain the mechanism by which Atg7 transfers Atg8 and Atg12 to E2 enzymes (42, 123). The Atg7-Atg3 and Atg7-Atg10 interactions are similar to each other yet distinct from canonical E1-E2 interactions

(31). Both Atg3 and Atg10 are wedged between the NTD and CTD of Atg7 and interact with β15 of the Atg7 NTD using the same loop region that follows β4 (**Figure 3c**). The loop region of Atg10 forms an intermolecular β-sheet with Atg7 β15, whereas in the case of Atg3 no such β-sheet is formed and the interactions are mediated mainly by side chains. In addition, the short helix in Atg3^{FR} is bound to the hydrophobic shoulder groove in the Atg7 NTD (**Figure 3d**). The catalytic cysteine of both Atg3 and Atg10 is positioned distal to the catalytic Cys507 of the Atg7 protomer to which Atg3 and Atg10 are bound, but much nearer to the Cys507 of the other Atg7 protomer within a dimer (**Figure 3d**). This suggests that both Atg8 and Atg12 are transferred from the Cys507 of one Atg7 protomer to the catalytic cysteine of the cognate E2 bound to the other Atg7 protomer within a dimer. This *trans* reaction model, which was confirmed by biochemical studies using heterodimerized Atg7 mutants (86, 116), is unique to Atg7 among E1 enzymes and explains why the homodimer architecture is essential for Atg7's functions. Atg7 transfers Atg8 to Atg3 and Atg12 to Atg10 in vivo; however, in vitro studies showed that Atg7 can transfer Atg8 to Atg10 and Atg12 to Atg3, and importantly that the transfer of Atg12 to Atg3 was more efficient than the transfer of Atg12 to Atg10 (123). Further studies are required to determine the mechanisms that govern the specific formation of Atg8~Atg3 and Atg12~Atg10 thioester intermediates in vivo.

The Atg12-Atg5-Atg16 Complex: An E3-Like Enzyme

The Atg12-Atg5 conjugate forms a complex with Atg16 and functions as an E3-like enzyme in the Atg8 conjugation system (11, 14, 18, 72). In vitro studies have shown that the Atg12-Atg5 conjugate facilitates the transfer reaction of Atg8 from Atg3 to PE through a reorganization of the catalytic center of the E2-like enzyme Atg3 (99). Atg16 has no E3-like activity in vitro and its role in vivo is considered to target the Atg12-Atg5 conjugate to the autophagic membranes (14).

Crystallographic studies unveiled the unique architecture of the Atg12-Atg5-Atg16 complex, which is distinct from that of other E3 enzymes (12, 66, 81, 91, 115) (**Figure 3g**). Atg12 and Atg5 contain one and two ubiquitin folds, respectively, giving the Atg12-Atg5 conjugate a three-ubiquitin-fold architecture. Atg16 is composed of the Atg5-binding domain and the dimeric coiled-coil domain. As a result the Atg12-Atg5-Atg16 complex forms a 2:2:2 complex and thus contains six ubiquitin folds. However, the biological significance of this unique architecture remains to be established. In higher eukaryotes, Atg3^{FR} contains a motif that specifically binds Atg12 (68) (**Figure 3g**); thus, for Atg3, binding to Atg12 and Atg7 is mutually exclusive (95), whereas yeast Atg3 does not have such an Atg12-binding motif and the affinity between Atg3 and Atg12 is much lower than that between their human counterparts (K. Matoba & N.N. Noda, unpublished observations). The currently accepted model of the Atg8-PE conjugation mediated by the Atg12-Atg5-Atg16 complex is as follows: The Atg12-Atg5-Atg16 complex targets the autophagic membrane via the Atg5-Atg16 complex moiety and then recruits a Atg3~Atg8 thioester intermediate via the interaction between Atg3 and Atg12. These interactions play at least two roles in the reaction: One role is to activate the catalytic site of Atg3 (99) and the other is to locate the Atg3~Atg8 thioester near the PE. Structural studies on the full-length E2-E3 complex are needed to uncover the molecular mechanisms of this unique conjugation reaction.

PAS-Targeting Mechanism of Atg Conjugation Systems

The original hierarchy map showed that the Atg conjugation systems depend on the PI3K complex but not the Atg2-Atg18 complex to target the PAS (113). However, studies using fission yeast have shown that Atg8 depends on Atg18a to target the PAS and that Atg18a interacts with Atg5,

which leads to a proposed model in which Atg18a recruits Atg8 to the PAS through the Atg12-Atg5-Atg16 complex (109). Further, studies of mammalian autophagy have shown that an Atg18 homolog, WIPI2b, interacts directly with the mammalian Atg16 ortholog, Atg16L1, and that this interaction is essential for autophagy (10). Furthermore, Atg18-family proteins target to the PAS by binding to PI3P (phosphatidylinositol 3-phosphate), which is produced by PI3K (74). These data indicate that Atg18-family proteins that localize to the PAS by binding to PI3P directly recruit the Atg12-Atg5-Atg16 complex, which then recruits Atg8 to the PAS.

Crystallographic studies have shown in detail the architecture of Atg18 on an Atg18 paralog, Hsv2 (3, 56, 119) (**Figure 3***g*). Hsv2 has a seven-bladed β-propeller fold and possesses two binding pockets for PI3P at blades 5 and 6. Both WIPI2b and Atg18 utilize blade 2 to interact with Atg16L1 and Atg2, respectively (10, 119). Therefore, Atg2 and Atg16 may compete to bind to Atg18 if both proteins can bind to the same Atg18 paralog. Alternatively, each Atg18 paralog might have a specific binding partner: one specific to Atg2 and another specific to Atg16. In *S. cerevisiae*, there are three Atg18 paralogs: Atg18, Atg21, and Hsv2. Although only Atg18 is essential for autophagy, Atg18 and Atg21 cooperate to recruit Atg8 to the PAS (76). Detailed functional and structural studies are needed to establish the molecular role of each paralog in autophagy.

CONCLUDING REMARKS

Structural biological studies on core Atg proteins, especially those forming the Atg1 complex and the Atg conjugation systems, have developed rapidly. However, the structures of the protein Atg9, the Atg2-Atg18 complex, and the PI3K complex have yet to be fully unveiled. Furthermore, most of the interactions connecting the six functional groups are poorly understood. A determination of the structures of all core Atg proteins and the critical interactions among them would serve as a powerful compass to guide researchers toward a better understanding of the molecular mechanisms in autophagy.

SUMMARY POINTS

1. Atg1 and Atg13 have elongated KD-IDR-MIT and HORMA-IDR architectures, respectively, whereas Atg17 has a unique S-shaped architecture.

2. The Atg13 IDR binds directly to Atg1 MIT using MIM and to Atg17 using a short sequence.

3. Upon starvation, the interaction of Atg13 with both Atg1 and Atg17 is enhanced by dephosphorylation at specific serines in Atg13, leading to the formation of the Atg1 complex.

4. Atg4 has a papain-like fold with unique insertions that enable specific recognition and delipidation of Atg8.

5. Atg7 (E1), Atg3 (E2), and Atg10 (E2) in Atg conjugation systems possess both canonical and noncanonical structural features and mediate the activation reaction of Atg8 and Atg12 with a unique *trans* mechanism.

6. The Atg12-Atg5-Atg16 complex (E3), which is not structurally similar to other E3 enzymes, mediates both activation and membrane-targeting of Atg3 for Atg8 lipidation.

DISCLOSURE STATEMENT

The authors are not aware of any affiliations, memberships, funding, or financial holdings that might be perceived as affecting the objectivity of this review.

ACKNOWLEDGMENTS

LITERATURE CITED

1. Araki Y, Ku WC, Akioka M, May AI, Hayashi Y, et al. 2013. Atg38 is required for autophagy-specific phosphatidylinositol 3-kinase complex integrity. *J. Cell Biol.* 203:299–313

2. Aravind L, Koonin EV. 1998. The HORMA domain: a common structural denominator in mitotic checkpoints, chromosome synapsis and DNA repair. *Trends Biochem. Sci.* 23:284–86

3. Baskaran S, Ragusa MJ, Boura E, Hurley JH. 2012. Two-site recognition of phosphatidylinositol 3-phosphate by PROPPINs in autophagy. *Mol. Cell* 47:339–48

4. Bodenmiller B, Wanka S, Kraft C, Urban J, Campbell D, et al. 2010. Phosphoproteomic analysis reveals interconnected system-wide responses to perturbations of kinases and phosphatases in yeast. *Sci. Signal.* 3:rs4

5. Budovskaya YV, Stephan JS, Deminoff SJ, Herman PK. 2005. An evolutionary proteomics approach identifies substrates of the cAMP-dependent protein kinase. *PNAS* 102:13933–38

6. Chan EY, Longatti A, McKnight NC, Tooze SA. 2009. Kinase-inactivated ULK proteins inhibit autophagy via their conserved C-terminal domains using an Atg13-independent mechanism. *Mol. Cell. Biol.* 29:157–71

7. Cheong H, Nair U, Geng J, Klionsky DJ. 2008. The Atg1 kinase complex is involved in the regulation of protein recruitment to initiate sequestering vesicle formation for nonspecific autophagy in *Saccharomyces cerevisiae*. *Mol. Biol. Cell* 19:668–81

8. Cheong H, Yorimitsu T, Reggiori F, Legakis JE, Wang CW, Klionsky DJ. 2005. Atg17 regulates the magnitude of the autophagic response. *Mol. Biol. Cell* 16:3438–53

9. Chew LH, Setiaputra D, Klionsky DJ, Yip CK. 2013. Structural characterization of the *Saccharomyces cerevisiae* autophagy regulatory complex Atg17-Atg31-Atg29. *Autophagy* 9:1467–74

10. Dooley HC, Razi M, Polson HEJ, Girardin SE, Wilson MI, Tooze SA. 2014. WIPI2 links LC3 conjugation with PI3P, autophagosome formation, and pathogen clearance by recruiting Atg12–5-16L1. *Mol. Cell* 55:238–52

11. Fujioka Y, Noda NN, Fujii K, Yoshimoto K, Ohsumi Y, Inagaki F. 2008. In vitro reconstitution of plant Atg8 and Atg12 conjugation systems essential for autophagy. *J. Biol. Chem.* 283:1921–28

12. Fujioka Y, Noda NN, Nakatogawa H, Ohsumi Y, Inagaki F. 2010. Dimeric coiled-coil structure of *Saccharomyces cerevisiae* Atg16 and its functional significance in autophagy. *J. Biol. Chem.* 285:1508–15

13. Fujioka Y, Suzuki SW, Yamamoto H, Kondo-Kakuta C, Kimura Y, et al. 2014. Structural basis of starvation-induced assembly of the autophagy initiation complex. *Nat. Struct. Mol. Biol.* 21:513–21

14. Fujita N, Itoh T, Omori H, Fukuda M, Noda T, Yoshimori T. 2008. The Atg16L complex specifies the site of LC3 lipidation for membrane biogenesis in autophagy. *Mol. Biol. Cell* 19:2092–100

15. Ganley IG, Lam DH, Wang J, Ding X, Chen S, Jiang X. 2009. ULK1·ATG13·FIP200 complex mediates mTOR signaling and is essential for autophagy. *J. Biol. Chem.* 284:12297–305

16. Gnad F, de Godoy LMF, Cox J, Neuhauser N, Ren S, et al. 2009. High-accuracy identification and bioinformatic analysis of in vivo protein phosphorylation sites in yeast. *Proteomics* 9:4642–52

17. Hain AU, Weltzer RR, Hammond H, Jayabalasingham B, Dinglasan RR, et al. 2012. Structural charac- terization and inhibition of the *Plasmodium* Atg8-Atg3 interaction. *J. Struct. Biol.* 180:551–62

18. Hanada T, Noda NN, Satomi Y, Ichimura Y, Fujioka Y, et al. 2007. The Atg12-Atg5 conjugate has a novel E3-like activity for protein lipidation in autophagy. *J. Biol. Chem.* 282:37298–302

19. Hanada T, Satomi Y, Takao T, Ohsumi Y. 2009. The amino-terminal region of Atg3 is essential for association with phosphatidylethanolamine in Atg8 lipidation. *FEBS Lett.* 583:1078–83

20. Hara T, Takamura A, Kishi C, Iemura S, Natsume T, et al. 2008. FIP200, a ULK-interacting protein, is required for autophagosome formation in mammalian cells. *J. Cell Biol.* 181:497–510

21. He C, Baba M, Cao Y, Klionsky DJ. 2008. Self-interaction is critical for Atg9 transport and function at the phagophore assembly site during autophagy. *Mol. Biol. Cell* 19:5506–16

22. Hecker C-M, Rabiller M, Haglund K, Bayer P, Dikic I. 2006. Specification of SUMO1- and SUMO2- interacting motifs. *J. Biol. Chem.* 281:16117–27

23. Hegedűs K, Ńagy P, Gáspári Z, Juhász G. 2014. The putative HORMA domain protein Atg101 dimerizes and is required for starvation-induced and selective autophagy in *Drosophila*. *BioMed Res. Int.* 2014:470482

24. Helbig AO, Rosati S, Pijnappel PW, van Breukelen B, Timmers MH, et al. 2010. Perturbation of the yeast *N*-acetyltransferase NatB induces elevation of protein phosphorylation levels. *BMC Genomics* 11:685

25. Hong SB, Kim BW, Kim JH, Song HK. 2012. Structure of the autophagic E2 enzyme Atg10. *Acta Crystallogr. D* 68:1409–17

26. Hong SB, Kim BW, Lee KE, Kim SW, Jeon H, et al. 2011. Insights into noncanonical E1 enzyme activation from the structure of autophagic E1 Atg7 with Atg8. *Nat. Struct. Mol. Biol.* 18:1323–30

27. Hosokawa N, Hara T, Kaizuka T, Kishi C, Takamura A, et al. 2009. Nutrient-dependent mTORC1 association with the ULK1-Atg13-FIP200 complex required for autophagy. *Mol. Biol. Cell* 20:1981–91

28. Hosokawa N, Hara Y, Mizushima N. 2006. Generation of cell lines with tetracycline-regulated autophagy and a role for autophagy in controlling cell size. *FEBS Lett.* 580:2623–29

29. Hosokawa N, Sasaki T, Iemura S, Natsume T, Hara T, Mizushima N. 2009. Atg101, a novel mammalian autophagy protein interacting with Atg13. *Autophagy* 5:973–79

30. Hu C, Zhang X, Teng YB, Hu HX, Li WF. 2010. Structure of autophagy-related protein Atg8 from the silkworm *Bombyx mori*. *Acta Crystallogr. F* 66:787–90

31. Huang DT, Paydar A, Zhuang M, Waddell MB, Holton JM, Schulman BA. 2005. Structural basis for recruitment of Ubc12 by an E2 binding domain in NEDD8's E1. *Mol. Cell* 17:341–50

32. Huber A, Bodenmiller B, Uotila A, Stahl M, Wanka S, et al. 2009. Characterization of the rapamycin- sensitive phosphoproteome reveals that Sch9 is a central coordinator of protein synthesis. *Genes Dev.* 23:1929–43

33. Hurley JH, Schulman BA. 2014. Atomistic autophagy: the structures of cellular self-digestion. *Cell* 157:300–11

34. Hurley JH, Yang D. 2008. MIT domainia. *Dev. Cell* 14:6–8

35. Ichimura Y, Kirisako T, Takao T, Satomi Y, Shimonishi Y, et al. 2000. A ubiquitin-like system mediates protein lipidation. *Nature* 408:488–92

36. Ichimura Y, Kumanomidou T, Sou YS, Mizushima T, Ezaki J, et al. 2008. Structural basis for sorting mechanism of p62 in selective autophagy. *J. Biol. Chem.* 283:22847–57

37. Jao CC, Ragusa MJ, Stanley RE, Hurley JH. 2013. A HORMA domain in Atg13 mediates PI 3-kinase recruitment in autophagy. *PNAS* 110:5486–91

38. Jung CH, Jun CB, Ro S-H, Kim Y-M, Otto NM, et al. 2009. ULK-Atg13-FIP200 complexes mediate mTOR signaling to the autophagy machinery. *Mol. Biol. Cell* 20:1992–2003

39. Kabeya Y, Kamada Y, Baba M, Takikawa H, Sasaki M, Ohsumi Y. 2005. Atg17 functions in cooperation with Atg1 and Atg13 in yeast autophagy. *Mol. Biol. Cell* 16:2544–53

40. Kabeya Y, Mizushima N, Yamamoto A, Oshitani-Okamoto S, Ohsumi Y, Yoshimori T. 2004. LC3, GABARAP and GATE16 localize to autophagosomal membrane depending on form-II formation. *J. Cell Sci.* 117:2805–12

41. Kabeya Y, Noda NN, Fujioka Y, Suzuki K, Inagaki F, Ohsumi Y. 2009. Characterization of the Atg17-Atg29-Atg31 complex specifically required for starvation-induced autophagy in *Saccharomyces cerevisiae*. *Biochem. Biophys. Res. Commun.* 389:612–15

42. Kaiser SE, Mao K, Taherbhoy AM, Yu S, Olszewski JL, et al. 2012. Noncanonical E2 recruitment by the autophagy E1 revealed by Atg7-Atg3 and Atg7-Atg10 structures. *Nat. Struct. Mol. Biol.* 19:1242–49

43. Kamada Y, Funakoshi T, Shintani T, Nagano K, Ohsumi M, Ohsumi Y. 2000. Tor-mediated induction of autophagy via an Apg1 protein kinase complex. *J. Cell Biol.* 150:1507–13

44. Kamada Y, Yoshino K, Kondo C, Kawamata T, Oshiro N, et al. 2010. Tor directly controls the Atg1 kinase complex to regulate autophagy. *Mol. Cell. Biol.* 30:1049–58

45. Kaufmann A, Beier V, Franquelim HG, Wollert T. 2014. Molecular mechanism of autophagic membrane-scaffold assembly and disassembly. *Cell* 156:469–81

46. Kawamata T, Kamada Y, Kabeya Y, Sekito T, Ohsumi Y. 2008. Organization of the pre-autophagosomal structure responsible for autophagosome formation. *Mol. Biol. Cell* 19:2039–50

47. Kihara A, Noda T, Ishihara N, Ohsumi Y. 2001. Two distinct Vps34 phosphatidylinositol 3-kinase complexes function in autophagy and carboxypeptidase Y sorting in *Saccharomyces cerevisiae*. *J. Cell Biol.* 152:519–30

48. Kijanska M, Dohnal I, Reiter W, Kaspar S, Stoffel I, et al. 2010. Activation of Atg1 kinase in autophagy by regulated phosphorylation. *Autophagy* 6:1168–78

49. Kim J, Kamada Y, Stromhaug PE, Guan J, Hefner-Gravink A, et al. 2001. Cvt9/Gsa9 functions in sequestering selective cytosolic cargo destined for the vacuole. *J. Cell Biol.* 153:381–96

50. Kirisako T, Ichimura Y, Okada H, Kabeya Y, Mizushima N, et al. 2000. The reversible modification regulates the membrane-binding state of Apg8/Aut7 essential for autophagy and the cytoplasm to vacuole targeting pathway. *J. Cell Biol.* 151:263–76

51. Klionsky DJ, Cregg JM, Dunn WA Jr, Emr SD, Sakai Y, et al. 2003. A unified nomenclature for yeast autophagy-related genes. *Dev. Cell* 5:539–45

52. Klionsky DJ, Schulman BA. 2014. Dynamic regulation of macroautophagy by distinctive ubiquitin-like proteins. *Nat. Struct. Mol. Biol.* 21:336–45

53. Kondo-Okamoto N, Noda NN, Suzuki SW, Nakatogawa H, Takahashi I, et al. 2012. Autophagy-related protein 32 acts as autophagic degron and directly initiates mitophagy. *J. Biol. Chem.* 287:10631–38

54. Koopmann R, Muhammad K, Perbandt M, Betzel C, Duszenko M. 2009. *Trypanosoma brucei* ATG8: structural insights into autophagic-like mechanisms in protozoa. *Autophagy* 5:1085–91

55. Kraft C, Kijanska M, Kalie E, Siergiejuk E, Lee SS, et al. 2012. Binding of the Atg1/ULK1 kinase to the ubiquitin-like protein Atg8 regulates autophagy. *EMBO J.* 31:3691–703

56. Krick R, Busse RA, Scacioc A, Stephan M, Janshoff A, et al. 2012. Structural and functional characterization of the two phosphoinositide binding sites of PROPPINs, a β-propeller protein family. *PNAS* 109:E2042–49

57. Kumanomidou T, Mizushima T, Komatsu M, Suzuki A, Tanida I, et al. 2006. The crystal structure of human Atg4b, a processing and de-conjugating enzyme for autophagosome-forming modifiers. *J. Mol. Biol.* 355:612–18

58. Kumeta H, Watanabe M, Nakatogawa H, Yamaguchi M, Ogura K, et al. 2010. The NMR structure of the autophagy-related protein Atg8. *J. Biomol. NMR* 47:237–41

59. Lamb CA, Yoshimori T, Tooze SA. 2013. The autophagosome: origins unknown, biogenesis complex. *Nat. Rev. Mol. Cell Biol.* 14:759–74

60. Levine B, Mizushima N, Virgin HW. 2011. Autophagy in immunity and inflammation. *Nature* 469:323–35

61. Li X, Gerber SA, Rudner AD, Beausoleil SA, Haas W, et al. 2007. Large-scale phosphorylation analysis of α-factor-arrested *Saccharomyces cerevisiae*. *J. Proteome Res.* 6:1190–97

62. Lu K, Psakhye I, Jentsch S. 2014. Autophagic clearance of polyQ proteins mediated by ubiquitin-Atg8 adaptors of the conserved CUET protein family. *Cell* 158:549–63

63. Luo X, Yu H. 2008. Protein metamorphosis: the two-state behavior of Mad2. *Structure* 16:1616–25

64. Lynch-Day MA, Klionsky DJ. 2010. The Cvt pathway as a model for selective autophagy. *FEBS Lett.* 584:1359–66

65. Mao K, Chew LH, Inoue-Aono Y, Cheong H, Nair U, et al. 2013. Atg29 phosphorylation regulates coordination of the Atg17-Atg31-Atg29 complex with the Atg11 scaffold during autophagy initiation. *PNAS* 110:E2875–84

66. Matsushita M, Suzuki NN, Obara K, Fujioka Y, Ohsumi Y, Inagaki F. 2007. Structure of Atg5· Atg16, a complex essential for autophagy. *J. Biol. Chem.* 282:6763–72

67. Mercer CA, Kaliappan A, Dennis PB. 2009. A novel, human Atg13 binding protein, Atg101, interacts with ULK1 and is essential for macroautophagy. *Autophagy* 5:649–62

68. Metlagel Z, Otomo C, Takaesu G, Otomo T. 2013. Structural basis of ATG3 recognition by the autophagic ubiquitin-like protein ATG12. *PNAS* 110:18844–49

69. Mizushima N. 2010. The role of the Atg1/ULK1 complex in autophagy regulation. *Curr. Opin. Cell Biol.* 22:132–39

70. Mizushima N, Komatsu M. 2011. Autophagy: renovation of cells and tissues. *Cell* 147:728–41

71. Mizushima N, Kuma A, Kobayashi Y, Yamamoto A, Matsubae M, et al. 2003. Mouse Apg16L, a novel WD-repeat protein, targets to the autophagic isolation membrane with the Apg12-Apg5 conjugate. *J. Cell Sci.* 116:1679–88

72. Mizushima N, Noda T, Ohsumi Y. 1999. Apg16p is required for the function of the Apg12p-Apg5p conjugate in the yeast autophagy pathway. *EMBO J.* 18:3888–96

73. Mizushima N, Noda T, Yoshimori T, Tanaka Y, Ishii T, et al. 1998. A protein conjugation system essential for autophagy. *Nature* 395:395–98

74. Mizushima N, Yoshimori T, Ohsumi Y. 2011. The role of Atg proteins in autophagosome formation. *Annu. Rev. Cell Dev. Biol.* 27:107–32

75. Motley AM, Nuttall JM, Hettema EH. 2012. Pex3-anchored Atg36 tags peroxisomes for degradation in *Saccharomyces cerevisiae*. *EMBO J.* 31:2852–68

76. Nair U, Cao Y, Xie Z, Klionsky DJ. 2010. Roles of the lipid-binding motifs of Atg18 and Atg21 in the cytoplasm to vacuole targeting pathway and autophagy. *J. Biol. Chem.* 285:11476–88

77. Nakatogawa H, Ichimura Y, Ohsumi Y. 2007. Atg8, a ubiquitin-like protein required for autophagosome formation, mediates membrane tethering and hemifusion. *Cell* 130:165–78

78. Nakatogawa H, Ohbayashi S, Sakoh-Nakatogawa M, Kakuta S, Suzuki SW, et al. 2012. The autophagy-related protein kinase Atg1 interacts with the ubiquitin-like protein Atg8 via the Atg8 family interacting motif to facilitate autophagosome formation. *J. Biol. Chem.* 287:28503–7

79. Nakatogawa H, Suzuki K, Kamada Y, Ohsumi Y. 2009. Dynamics and diversity in autophagy mechanisms: lessons from yeast. *Nat. Rev. Mol. Cell Biol.* 10:458–67

80. Nath S, Dancourt J, Shteyn V, Puente G, Fong WM, et al. 2014. Lipidation of the LC3/GABARAP family of autophagy proteins relies on a membrane-curvature-sensing domain in Atg3. *Nat. Cell Biol.* 16:415–24

81. Noda NN, Fujioka Y, Hanada T, Ohsumi Y, Inagaki F. 2013. Structure of the Atg12-Atg5 conjugate reveals a platform for stimulating Atg8-PE conjugation. *EMBO Rep.* 14:206–11

82. Noda NN, Kobayashi T, Adachi W, Fujioka Y, Ohsumi Y, Inagaki F. 2012. Structure of the novel C-terminal domain of vacuolar protein sorting 30/autophagy-related protein 6 and its specific role in autophagy. *J. Biol. Chem.* 287:16256–66

83. Noda NN, Kumeta H, Nakatogawa H, Satoo K, Adachi W, et al. 2008. Structural basis of target recognition by Atg8/LC3 during selective autophagy. *Genes Cells* 13:1211–18

84. Noda NN, Ohsumi Y, Inagaki F. 2009. ATG systems from the protein structural point of view. *Chem. Rev.* 109:1587–98

85. Noda NN, Ohsumi Y, Inagaki F. 2010. Atg8-family interacting motif crucial for selective autophagy. *FEBS Lett.* 584:1379–85

86. Noda NN, Satoo K, Fujioka Y, Kumeta H, Ogura K, et al. 2011. Structural basis of Atg8 activation by a homodimeric E1, Atg7. *Mol. Cell* 44:462–75

87. Noda T, Ohsumi Y. 1998. Tor, a phosphatidylinositol kinase homologue, controls autophagy in yeast. *J. Biol. Chem.* 273:3963–66

88. Novak I, Kirkin V, McEwan DG, Zhang J, Wild P, et al. 2010. Nix is a selective autophagy receptor for mitochondrial clearance. *EMBO Rep.* 11:45–51

89. Obara K, Sekito T, Ohsumi Y. 2006. Assortment of phosphatidylinositol 3-kinase complexes–Atg14p directs association of complex I to the pre-autophagosomal structure in *Saccharomyces cerevisiae*. *Mol. Biol. Cell* 17:1527–39

90. Ohsumi Y. 2001. Molecular dissection of autophagy: two ubiquitin-like systems. *Nat. Rev.* 2:211–16

91. Otomo C, Metlagel Z, Takaesu G, Otomo T. 2013. Structure of the human ATG12∼ATG5 conjugate required for LC3 lipidation in autophagy. *Nat. Struct. Mol. Biol.* 20:59–66

92. Pankiv S, Clausen TH, Lamark T, Brech A, Bruun J-A, et al. 2007. p62/SQSTM1 binds directly to Atg8/LC3 to facilitate degradation of ubiquitinated protein aggregates by autophagy. *J. Biol. Chem.* 282:24131–45

93. Papinski D, Schuschnig M, Reiter W, Wilhelm L, Barnes CA, et al. 2014. Early steps in autophagy depend on direct phosphorylation of Atg9 by the Atg1 kinase. *Mol. Cell* 53:471–83

94. Paz Y, Elazar Z, Fass D. 2000. Structure of GATE-16, membrane transport modulator and mammalian ortholog of autophagocytosis factor Aut7p. *J. Biol. Chem.* 275:25445–50

95. Qiu Y, Hofmann K, Coats JE, Schulman BA, Kaiser SE. 2013. Binding to E1 and E3 is mutually exclusive for the human autophagy E2 Atg3. *Protein Sci.* 22:1691–97

96. Ragusa MJ, Stanley RE, Hurley JH. 2012. Architecture of the Atg17 complex as a scaffold for autophagosome biogenesis. *Cell* 151:1501–12

97. Reggiori F, Tucker KA, Stromhaug PE, Klionsky DJ. 2004. The Atg1-Atg13 complex regulates Atg9 and Atg23 retrieval transport from the pre-autophagosomal structure. *Dev. Cell* 6:79–90

98. Rubinsztein DC, Shpilka T, Elazar Z. 2012. Mechanisms of autophagosome biogenesis. *Curr. Biol.* 22:R29–34

99. Sakoh-Nakatogawa M, Matoba K, Asai E, Kirisako H, Ishii J, et al. 2013. Atg12-Atg5 conjugate enhances E2 activity of Atg3 by rearranging its catalytic site. *Nat. Struct. Mol. Biol.* 20:433–39

100. Satoo K, Noda NN, Kumeta H, Fujioka Y, Mizushima N, et al. 2009. The structure of Atg4B-LC3 complex reveals the mechanism of LC3 processing and delipidation during autophagy. *EMBO J.* 28:1341–50

101. Schulman BA, Harper JW. 2009. Ubiquitin-like protein activation by E1 enzymes: the apex for downstream signaling pathways. *Nat. Rev. Mol. Cell Biol.* 10:319–31

102. Scott SV, Guan J, Hutchins MU, Kim J, Klionsky DJ. 2001. Cvt19 is a receptor for the cytoplasm-to-vacuole targeting pathway. *Mol. Cell* 7:1131–41

103. Shintani T, Mizushima N, Ogawa Y, Matsuura A, Noda T, Ohsumi Y. 1999. Apg10p, a novel protein-conjugating enzyme essential for autophagy in yeast. *EMBO J.* 18:5234–41

104. Soufi B, Kelstrup CD, Stoehr G, Fröhlich F, Walther TC, Olsen JV. 2009. Global analysis of the yeast osmotic stress response by quantitative proteomics. *Mol. Biosyst.* 5:1337–46

105. Soulard A, Cremonesi A, Moes S, Schütz F, Jenö P, Hall MN. 2010. The rapamycin-sensitive phosphoproteome reveals that TOR controls protein kinase A toward some but not all substrates. *Mol. Biol. Cell* 21:3475–86

106. Stephan JS, Yeh YY, Ramachandran V, Deminoff SJ, Herman PK. 2009. The Tor and PKA signaling pathways independently target the Atg1/Atg13 protein kinase complex to control autophagy. *PNAS* 106:17049–54

107. Sugawara K, Suzuki NN, Fujioka Y, Mizushima N, Ohsumi Y, Inagaki F. 2004. The crystal structure of microtubule-associated protein light chain 3, a mammalian homologue of *Saccharomyces cerevisiae* Atg8. *Genes Cells* 9:611–18

108. Sugawara K, Suzuki NN, Fujioka Y, Mizushima N, Ohsumi Y, Inagaki F. 2005. Structural basis for the specificity and catalysis of human Atg4B responsible for mammalian autophagy. *J. Biol. Chem.* 280:40058–65

109. Sun LL, Li M, Suo F, Liu XM, Shen EZ, et al. 2013. Global analysis of fission yeast mating genes reveals new autophagy factors. *PLOS Genet.* 9:e1003715

110. Suzuki H, Tabata K, Morita E, Kawasaki M, Kato R, et al. 2014. Structural basis of the autophagy-related LC3/Atg13 LIR complex: recognition and interaction mechanism. *Structure* 22:47–58

111. Suzuki K, Kirisako T, Kamada Y, Mizushima N, Noda T, Ohsumi Y. 2001. The pre-autophagosomal structure organized by concerted functions of APG genes is essential for autophagosome formation. *EMBO J.* 20:5971–81

112. Suzuki K, Kondo C, Morimoto M, Ohsumi Y. 2010. Selective transport of α-mannosidase by autophagic pathways: identification of a novel receptor, Atg34p. *J. Biol. Chem.* 285:30019–25

113. Suzuki K, Kubota Y, Sekito T, Ohsumi Y. 2007. Hierarchy of Atg proteins in pre-autophagosomal structure organization. *Genes Cells* 12:209–18

114. Suzuki K, Ohsumi Y. 2010. Current knowledge of the pre-autophagosomal structure (PAS). *FEBS Lett.* 584:1280–86

115. Suzuki NN, Yoshimoto K, Fujioka Y, Ohsumi Y, Inagaki F. 2005. The crystal structure of plant ATG12 and its biological implication in autophagy. *Autophagy* 1:119–26

116. Taherbhoy AM, Tait SW, Kaiser SE, Williams AH, Deng A, et al. 2011. Atg8 transfer from Atg7 to Atg3: a distinctive E1-E2 architecture and mechanism in the autophagy pathway. *Mol. Cell* 44:451–61

117. Thumm M, Egner R, Koch B, Schlumpberger M, Straub M, et al. 1994. Isolation of autophagocytosis mutants of *Saccharomyces cerevisiae*. *FEBS Lett.* 349:275–80

118. Tsukada M, Ohsumi Y. 1993. Isolation and characterization of autophagy-defective mutants of *Saccharomyces cerevisiae*. *FEBS Lett.* 333:169–74

119. Watanabe Y, Kobayashi T, Yamamoto H, Hoshida H, Akada R, et al. 2012. Structure-based analyses reveal distinct binding sites for Atg2 and phosphoinositides in Atg18. *J. Biol. Chem.* 287:31681–90

120. Weidberg H, Shpilka T, Shvets E, Abada A, Shimron F, Elazar Z. 2011. LC3 and GATE-16 N termini mediate membrane fusion processes required for autophagosome biogenesis. *Dev. Cell* 20:444–54

121. Xie Z, Nair U, Klionsky DJ. 2008. Atg8 controls phagophore expansion during autophagosome formation. *Mol. Biol. Cell* 19:3290–98

122. Yamada Y, Suzuki NN, Hanada T, Ichimura Y, Kumeta H, et al. 2007. The crystal structure of Atg3, an autophagy-related ubiquitin carrier protein (E2) enzyme that mediates Atg8 lipidation. *J. Biol. Chem.* 282:8036–43

123. Yamaguchi M, Matoba K, Sawada R, Fujioka Y, Nakatogawa H, et al. 2012. Noncanonical recognition and UBL loading of distinct E2s by autophagy-essential Atg7. *Nat. Struct. Mol. Biol.* 19:1250–56

124. Yamaguchi M, Noda NN, Nakatogawa H, Kumeta H, Ohsumi Y, Inagaki F. 2010. Autophagy-related protein 8 (Atg8) family interacting motif in Atg3 mediates the Atg3-Atg8 interaction and is crucial for the cytoplasm-to-vacuole targeting pathway. *J. Biol. Chem.* 285:29599–607

125. Yamaguchi M, Noda NN, Yamamoto H, Shima T, Kumeta H, et al. 2012. Structural insights into Atg10-mediated formation of the autophagy-essential Atg12-Atg5 conjugate. *Structure* 20:1244–54

126. Yamamoto H, Kakuta S, Watanabe TM, Kitamura A, Sekito T, et al. 2012. Atg9 vesicles are an important membrane source during early steps of autophagosome formation. *J. Cell Biol.* 198:219–33

127. Yeh YY, Shah KH, Herman PK. 2011. An Atg13 protein-mediated self-association of the Atg1 protein kinase is important for the induction of autophagy. *J. Biol. Chem.* 286:28931–39

128. Yeh YY, Wrasman K, Herman PK. 2010. Autophosphorylation within the Atg1 activation loop is required for both kinase activity and the induction of autophagy in *Saccharomyces cerevisiae*. *Genetics* 185:871–82